DOI: 10.1002/cbic.200700555

Development of Bacteriophage P22 as a Platform for Molecular Display: Genetic and Chemical Modifications of the Procapsid Exterior Surface

Sebyung Kang,[a] Gabriel C. Lander,[b] John E. Johnson,[b] and Peter E. Prevelige*[a]

Virus capsids are composed of hundreds of copies of a small number of protein subunits which not only self-assemble into precise and uniform viral capsids but which also have remarkable plasticity allowing viruses to undergo concerted conformational changes during their life cycle[1–3] as well as to adapt to environmental stresses such as pH and salts.[4,5] The protein cage architecture of viral capsids provides both interior and exterior surfaces for chemical and genetic manipulation.[6–12]

The *Salmonella typhimurium* bacteriophage P22 has potential to serve as a platform for molecular devices. Bacteriophage P22 derived virus-like particles are relatively easy to obtain in quantity (by overexpression 100 mg can be purified from one liter of culture), the life cycle is well understood genetically and biochemically, facilitating genetic manipulation,[13–16] and an in vitro assembly system is well established.[17,18] A $T=7$ P22 procapsid is assembled from 420 copies of the 46.6 kDa coat protein with the aid of approximately 300 copies of the 33.6 kDa scaffolding protein with a diameter of 58 nm (Figure 1).[18,19]

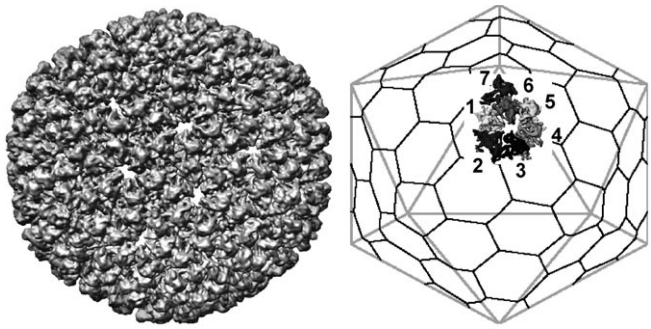

Figure 1. Outer surface representation of the 8.5 Å resolution density map of the $T=7$ P22 procapsid (left panel) and the asymmetric unit (right panel). Seven quasi-equivalent subunits are indicated on the asymmetric unit.

Previous limited proteolysis and mass spectrometry based hydrogen/deuterium exchange studies suggested that P22 procapsids have a flexible loop exposed to the surface of capsid[20,21] which represents a good locus for the attachment of functional groups, affinity tags, or quantum dots for surface presentation or targeting. The flexible nature of the loop allowed introduction of a cysteine residue in the middle of the loop region (T182C) without altering procapsid assembly or capsid integrity.[22] Cysteine residues (C182) engineered into the loop region were chemically reactive in the native form of procapsids (Figure S1 in the Supporting Information).

To test whether introduced cysteine residues can be selectively and covalently modified with cysteine reactive reagents, T182C procapsids were treated with MIANS (2-(4′-maleimidylanilino) naphthalene-6-sulfonic acid) which is a thiol reactive fluorescent probe absorbing at 322 nm wavelength.[23] Free MIANS exhibits little or no fluorescence in solution, but its fluorescence increases dramatically upon covalent attachment to a free sulfhydryl group.[24] The MIANS treated T182C procapsids were sedimented through a 5–20% sucrose velocity gradient and fractions were analyzed by SDS-PAGE. Wild-type and untreated T182C procapsids were sedimented in parallel and they sedimented to a similar position suggesting that covalent binding of MIANS to the T182C procapsids did not perturb shell integrity (Figure S2).

To estimate the extent of MIANS labeling the MIANS treated T182C procapsid fractions were collected and the absorption and fluorescence emission spectra were taken (Figure 2A and B). The number of MIANS molecules attached to the T182C procapsids was quantified by measuring the absorbance of the MIANS and the coat protein at 322 nm and 280 nm, respectively (Figure 2A). Approximately 345 MIANS molecules were bound per T182C procapsid (420 coat protein subunits) which translates to approximately 82% occupancy. It should be noted that there are 360 hexavalent subunits in the lattice suggesting that perhaps only the hexavalent subunits are reactive. Furthermore, a significant fluorescence intensity increase was observed with a maximum at 435 nm (excitation $\lambda=322$ nm) confirming the covalent nature of the attachment (Figure 2B).

Although the naturally occurring cysteine residue is buried and inactive (Figure S1), it is possible that MIANS modifies both the engineered and the naturally occurring cysteines. The extent of modification per subunit was determined by electrospray ionization time-of-flight mass spectrometry (ESI-TOF MS) (Figure 2C). Component analysis of the charge state distributions (Figure 2C) and its deconvolution (Figure 2C, inset) revealed that the dominant species in the MIANS treated T182C procapsid sample were a 47018.9 Da subunit (80%) and a 46623.2 Da subunit (20%). These masses are in excellent agreements with the values of 47017.1 Da and 46622.8 Da predicted for a coat protein subunit labeled with a single MIANS and the unlabeled subunit, respectively. No modification was observed when the wild-type protein was similarly

[a] *S. Kang, Prof. P. E. Prevelige*
Department of Microbiology, University of Alabama at Birmingham
BBRB 416 845 19thSt South, Birmingham, AL 35294-2170 (USA)
Fax: (+1) 205-975-5479
E-mail: prevelig@uab.edu

[b] *G. C. Lander, Prof. J. E. Johnson*
Department of Molecular Biology, The Scripps Research Institute
La Jolla, California 92037 (USA)

Supporting information for this article is available on the WWW under http://www.chembiochem.org or from the author.

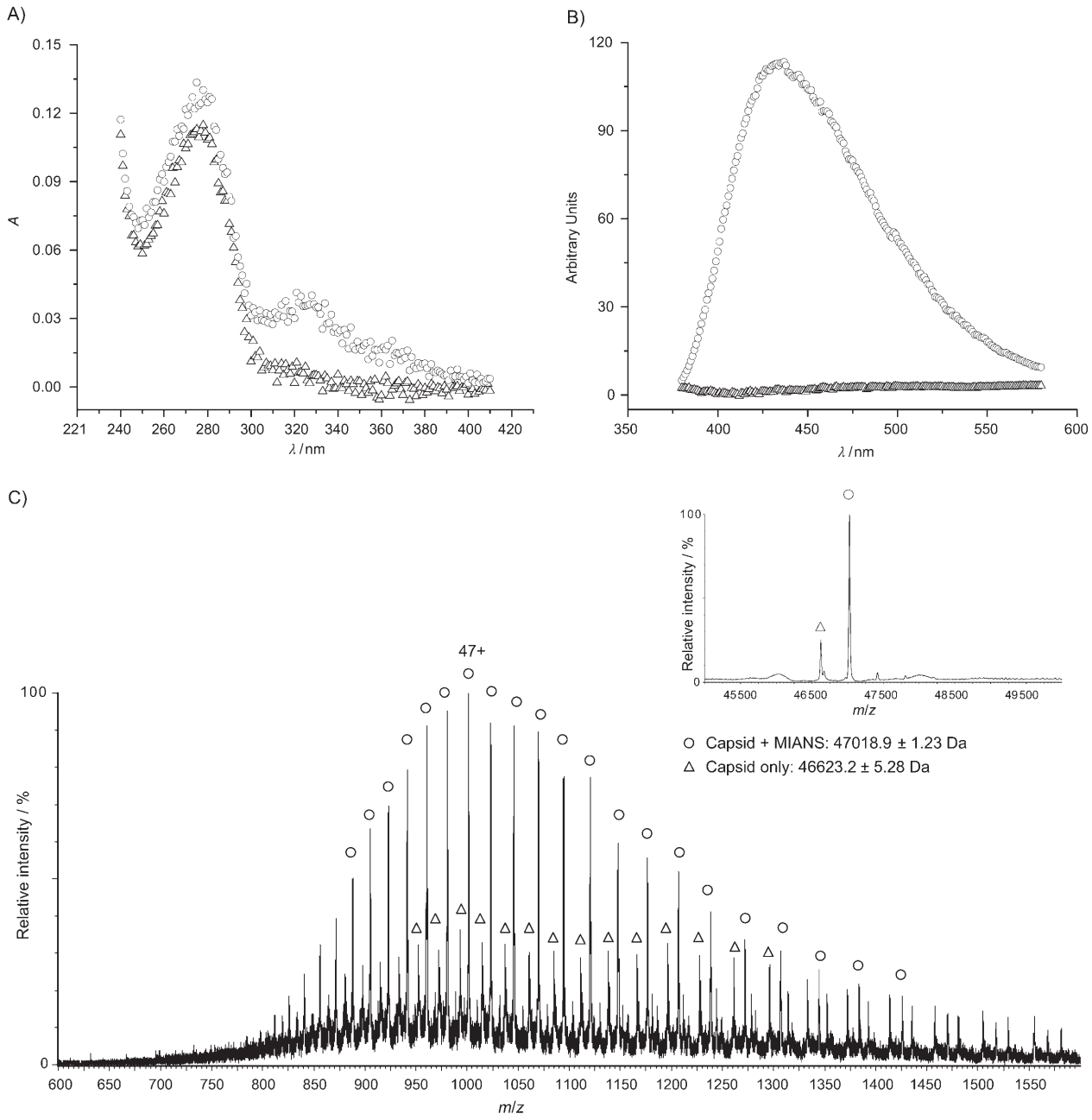

Figure 2. Spectroscopic and mass spectrometric analyses of the MIANS treated T182C procapsids. The T182C and the MIANS treated T182C procapsids were separated on a 5–20% sucrose gradient and fractions 5 and 6 (Figure S2B and C) were collected for further analysis. A) The absorption spectra of the T182C (△) and the MIANS treated T182C (○) procapsids were measured from 410 to 230 nm in buffer B supplemented with 6 M GuHCl. B) The fluorescence emission spectra of T182C (△) and MIANS treated T182C (○) procapsids (λ_{ex} = 322 nm) were obtained in buffer B. C) ESI-TOF mass spectrum of the dissociated subunits of the MIANS treated T182C procapsids. Two dominant Gaussian charge state distributions were labeled as open circles and triangles. Component analyses and deconvolution (inset) of two dominant charge state distributions showed masses of a single MIANS labeled (○, calcd 47017.1 Da; obs. 47018.9 Da) and the unlabeled (△, calcd 46622.8 Da; obs. 46623.2 Da) subunits. 47+ charged peak of a single MIANS labeled subunits is indicated.

treated. Therefore, the ESI-MS data is consistent with the spectroscopic analysis (Figure 2A) and confirms that MIANS only modifies C182.

We have also substituted T182 with other bulky hydrophobic amino acids (phenylalanine, tryptophan, and proline) and all the single amino acid substitution mutants produced procapsids without any assembly defects or morphological changes suggesting that the loop region is generally tolerant to amino acid substitutions (data not shown).

The affinity tag of six consecutive histidine residues (6X-His-tag) binds tightly to Ni ions and has been used extensively for metal chelate affinity based protein purification. To test whether P22 procapsids are tolerant to external sequence insertion, we introduced six consecutive histidines into the loop region

(6X-His-tag) by replacing T182 with the sequence GTHHHHHH. The 6X-His-tagged construct (HI) produced procapsid-like particles which migrated to the same position both on sucrose gradient and native agarose gels as did the wild type (data not shown).

To examine whether an inserted 6X-His-tag is exposed on the surface and accessible for noncovalent modification, we investigated the binding of a monoclonal antibody directed towards the 6X-His-tag antibody to the HI procapsids. The HI procapsids were incubated with anti-His-tag antibodies at 4 °C overnight, sedimented through a 5–20% sucrose gradient and analyzed by SDS-PAGE. The proteins were visualized by Coomasie blue staining (Figure 3A, B) and Western blotting using a secondary antibody directed towards the anti-His-tag antibodies (Figure 3C, D). Wild-type procapsids were used as control. The procapsids migrated at fractions 5, 6, and 7 in both the wild-type and the HI procapsids (Figure 3A, B). Anti-His-tag antibodies comigrated with the HI procapsids in fractions 5, 6, and 7, whereas they remained on the top of the gradient in the wild-type procapsid control suggesting that the antibodies are bound on the HI procapsid surfaces and that binding is specific (Figure 3C and D).

As the His-tags in the HI procapsids have high affinity against Ni ions, we attempted to label the HI procapsids with Ni-conjugated nanogold (1.8 nm diameter) and visualize them in the electron microscope. The HI procapsids were incubated with Ni-conjugated nanogold at a one to one molar ratio at 4 °C overnight. As a control, wild-type procapsids were treated in parallel. Ni-conjugated nanogold treated HI procapsids did not alter their integrity (Figure 4). As shown in Figure 4, there were no detectable electron-dense dots on the control wild-type procapsids and background (Figure 4A), whereas many such dots (arrow head) were detected on the HI procapsids (Figure 4B) suggesting that unbound Ni-conjugated nanogold is effectively removed by sucrose velocity gradient sedimentation and only the His-tag associated Ni-conjugated nanogold was observed.

In this study, we have demonstrated that the loop region of the P22 procapsid can be genetically modified and utilized for further chemical modifications providing a convenient mechanism to modify the outer surface of the procapsid.

Whereas a similar region has not been identified on the internal surface, the scaffolding protein can provide a facile mechanism for introducing internal modifications. The inner core of scaffolding protein in the P22 procapsids is stable but

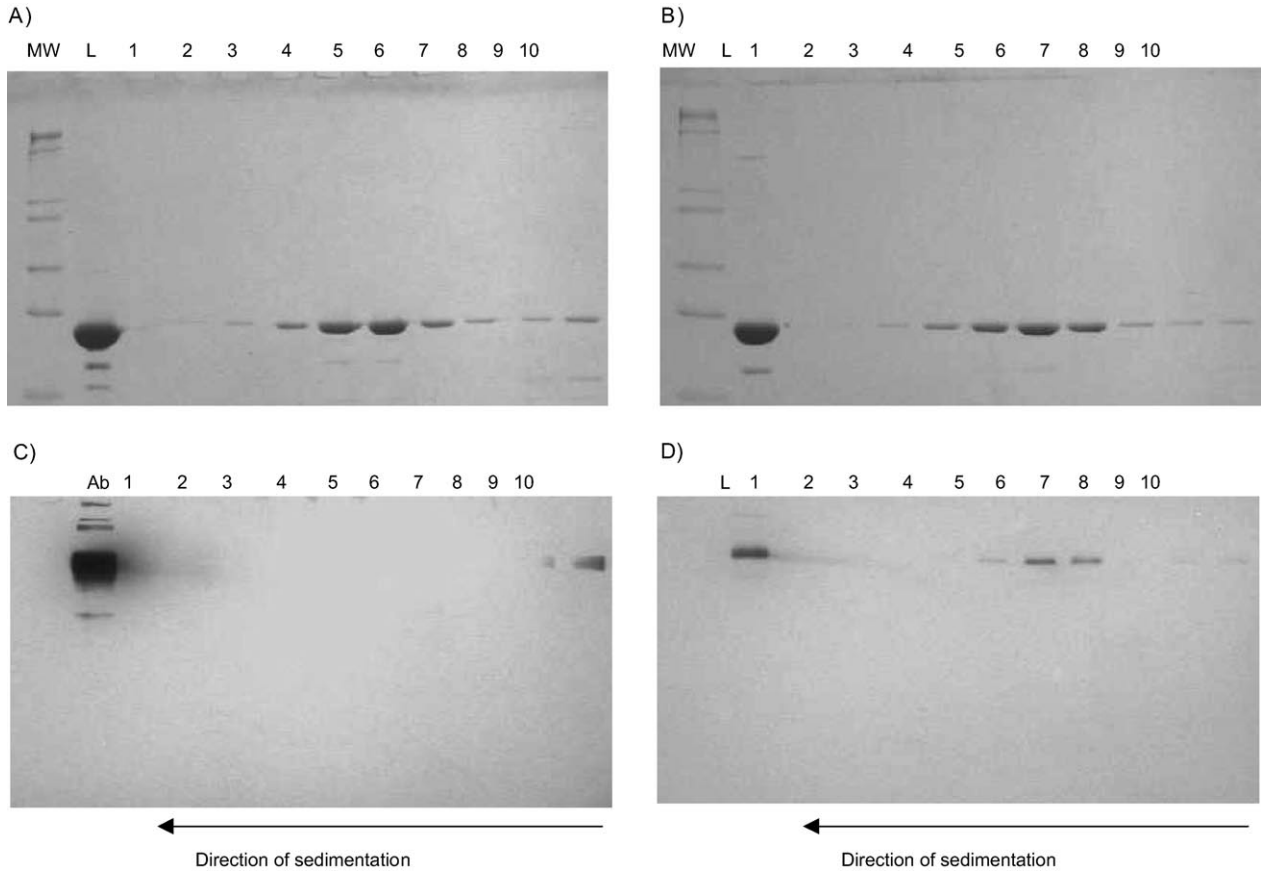

Figure 3. Sucrose velocity gradient sedimentations of anti-His-tag antibody treated wild-type and His-tag inserted (HI) procapsids. Wild-type and HI procapsids were incubated with anti-His-tag antibody at 4 °C overnight and separated on a 5–20% sucrose gradient. Fractions from the gradient were analyzed on duplicate 8.5% nonreducing SDS gels. Panels A) wild-type and B) HI procapsid fractions were stained with Coomassie blue. Panels C) wild-type and D) HI were electrophoretically transferred to PVDF membrane, blotted with alkaline phosphatase conjugated goat antimouse IgG, and visualized by reaction with the chromogenic substrate solution of 3-bromo-4-chloro-5-indolyl phosphate (BCIP) and nitro blue tetrazolium (NBT; Novagen).

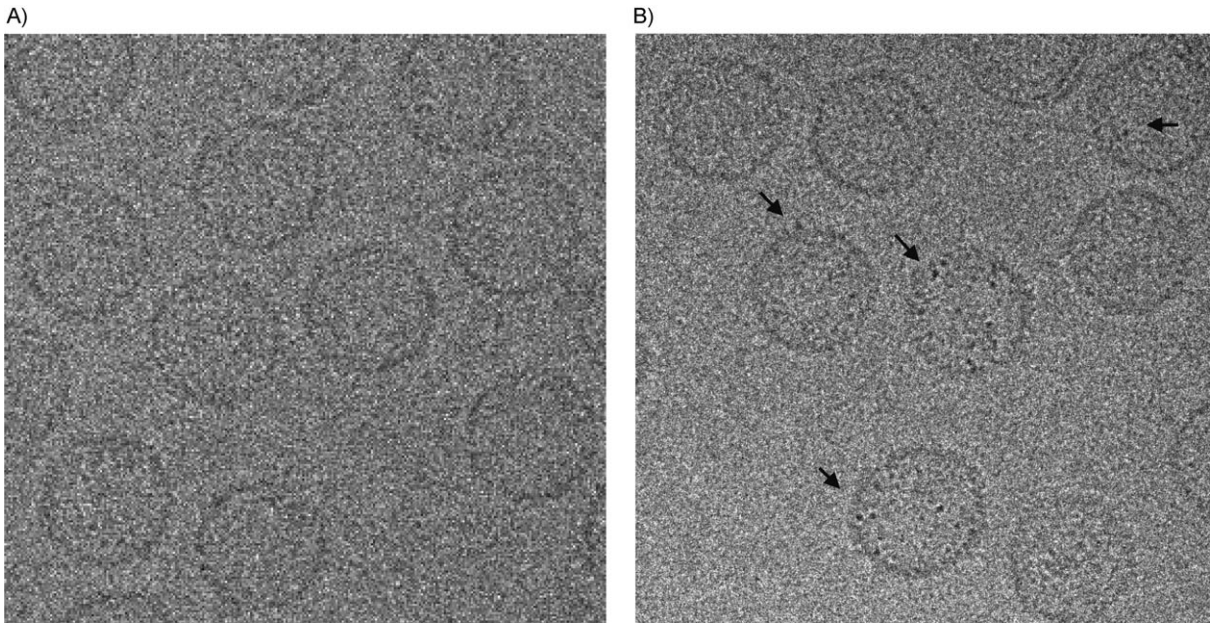

Figure 4. Cryoelectron micrographs of the Ni-conjugated nanogold treated wild-type and HI procapsids. Wild-type and HI procapsids were incubated with Ni-conjugated nanogold at 4 °C overnight. The reactions were fractionated on 5–20% sucrose velocity gradient, and the procapsid fractions were collected, and subjected to flash freezing on EM grids. A) Wild-type procapsids. B) HI procapsids. Arrow heads indicate electron dense gold particles.

can be reversibly extracted and re-entered in vitro without disturbing the procapsid lattice.[18,25–29] Modification and re-entry of the scaffolding protein coupled with external modification of the capsid surface thus provides a means to incorporate specific chemical entities or peptides of defined binding affinity within an externally modified shell. The ability to modify the two components in separate steps will facilitate the development of well-defined binary systems.

Experimental Section

Mutagenesis and procapsid purification: All of the mutants were generated by using established polymerase chain reaction protocols using pET-3a based plasmids encoding genes for scaffolding and coat proteins as templates.[22] The amplified DNAs were transformed into $CaCl_2$ treated competent *E. coli* strain BL21 (DE) and selected for ampicillin resistance. Mutant procapsids were overexpressed in *E. coli* and purified by sucrose gradient centrifugation as previously described.[22] The empty procapsids were prepared by repeated extraction of scaffolding protein with GuHCl (0.5 M) at 4 °C. Purified empty procapsids were stored in buffer B (50 mM Tris-HCl, 25 mM NaCl, and 2 mM EDTA) at 4 °C.

MIANS labeling of the T182C procapsids: The T182C procapsids (200 μM) were reduced with excess TCEP (2 mM) at room temperature for an hour and incubated with MIANS (2-(4′-maleimidylanilino) naphthalene-6-sulfonic acid) (2 mM) at 4 °C overnight. Reactions were fractionated by ultracentrifugation on a sucrose gradient (5–20%) with SW55 rotor (30,000 rpm for 35 min) and fractions were analyzed by SDS-PAGE and spectrophotometer. Absorption spectra of the fractions were recorded (20 °C) on Beckman DU 640 spectrophotometer over the spectral range 240–600 nm with 1 nm bandwidth using 1 cm path length cells. Fluorescence emission spectra were obtained (20 °C) using an ISS PC1 photon counting spectrofluorometer ($\lambda_{exc} = 322$ nm) over the spectral range 380–580 nm in 1 cm path length cells.

Mass spectrometry: Subunit masses of the MIANS treated T182C procapsids were analyzed by LC-ESI time-of-flight mass spectrometry (LCT, Micromass). The MIANS treated T182C procapsids were dissociated and denatured with urea (8 M) and loaded directly onto a C4 trap (Michrom BioResources, Inc.) which replaced the loading loop allowing for rapid washing with water to avoid introducing urea into the ESI source. The proteins were rapidly eluted with a acetonitrile gradient (5–95%, 36 μL min^{-1} flow rate) Spectra were acquired in the range of *m/z* 200–1650. Mass spectra were processed using the MaxEnt 1 algorithm and component analysis from MassLynx version 4.0 to obtain average masses from multiple charge state distributions.

The binding of a monoclonal antibody directed towards the 6X-His-tag antibody to the HI procapsids: Wild type and HI procapsids (20 μM) were incubated with His-tag monoclonal antibody (1.5 μg) (Novagen) at room temperature for an hour. Reactions were fractionated by ultracentrifugation on a sucrose gradient (5–20%) using an SW55 rotor (30,000 rpm for 35 min) and fractions were analyzed by SDS-PAGE. Proteins separated by SDS-PAGE were transferred to PVDF (PolyVinyliDene Fluoride) membrane using an electrophoretic tank transfer system. His-tag monoclonal antibody on the PVDF membrane was detected by His-tag AP Western Reagents (Novagen) following procedure provided by manufacturer.

Acknowledgement

This work was supported by NIH grant GM47980 (P.E.P). Some of the work presented here was conducted at the National Resource for Automated Molecular Microscopy which is supported by the National Institutes of Health though the National Center for Research Resources' P41 program (RR17573)

Keywords: nanoparticles · phage P22 · procapsids · surface display

[1] B. L. Trus, F. P. Booy, W. W. Newcomb, J. C. Brown, F. L. Homa, D. R. Thomsen, A. C. Steven, *J. Mol. Biol.* **1996**, *263*, 447–462.
[2] R. Lata, J. F. Conway, N. Cheng, R. L. Duda, R. W. Hendrix, W. R. Wikoff, J. E. Johnson, H. Tsuruta, A. C. Steven, *Cell* **2000**, *100*, 253–263.
[3] W. Jiang, Z. Li, Z. Zhang, M. L. Baker, P. E. Prevelige, Jr., W. Chiu, *Nat. Struct. Biol.* **2003**, *10*, 131–135.
[4] K. P. Incardona NL, *Biophys. J.* **1964**, *4*, 11–21.
[5] L. Wang, L. C. Lane, D. L. Smith, *Protein Sci.* **2001**, *10*, 1234–1243.
[6] T. Douglas, M. Young, *Science* **2006**, *312*, 873–875.
[7] M. Uchida, M. T. Klem, M. Allen, P. Suci, M. Flenniken, E. Gillitzer, Z. Varpness, L. O. Liepold, M. Young, T. Douglas, *Adv. Mater.* **2007**, *19*, 1025–1042.
[8] T. Douglas, M. Young, *Nature* **1998**, *393*, 152–155.
[9] T. Douglas, E. Strable, D. Willits, A. Aitouchen, M. Libera, M. Young, *Adv. Mater.* **2002**, *14*, 415–418.
[10] M. Knez, A. Bittner, F. Boes, C. Wege, H. Jeske, E. Mai, K. Kern, *Nano. Lett.* **2003**, *3*, 1079–1082.
[11] Q. Wang, T. Lin, J. E. Johnson, M. G. Finn, *Chem. Biol.* **2002**, *9*, 813–819.
[12] J. D. Lewis, G. Destito, A. Zijlstra, M. J. Gonzalez, J. P. Quigley, M. Manchester, H. Stuhlmann, *Nat. Med.* **2006**, *12*, 354–360.
[13] J. King, D. Botstein, S. Casjens, W. Earnshaw, S. Harrison, E. Lenk, *Philos. Trans. R. Soc. London Ser. B* **1976**, *276*, 37–49.
[14] J. King, S. Casjens, *Nature* **1974**, *251*, 112–119.
[15] S. Casjens, *Virus Structure and Assembly*, Jones and Bartlett, Boston, **1985**.
[16] D. Botstein, R. K. Russell, C. H: Waddell, *Virology* **1972**, 268–282.
[17] M. Fuller, J. King, *J. Mol. Biol.* **1982**, *156*, 633–665.
[18] P. E. Prevelige, Jr., D. Thomas, J. King, *J. Mol. Biol.* **1988**, *202*, 743–757.
[19] S. Casjens, J. King, *J. Supramol. Struct.* **1974**, *2*, 202–224.
[20] S. Kang, P. E. Prevelige, Jr., *J. Mol. Biol.* **2005**, *347*, 935–948.
[21] J. Lanman, R. Tuma, P. E. Prevelige, Jr., *Biochemistry* **1999**, *38*, 14614–14623.
[22] S. Kang, A. M. Hawkridge, K. L. Johnson, D. C. Muddiman, P. E. Prevelige, Jr., *J. Proteome Res.* **2006**, *5*, 370–377.
[23] V. Srinivas, B. Raman, K. S. Rao, T. Ramakrishna, C. Rao, *Mol. Vision* **2005**, *11*, 249–255.
[24] S. S. Gupte, L. K. Lane, *J. Biol. Chem.* **1979**, *254*, 10362–10369.
[25] M. Fuller, J. King, *Virology* **1981**, *112*, 529–547.
[26] M. H. Parker, W. F. Stafford, 3rd, P. E. Prevelige, Jr., *J. Mol. Biol.* **1997**, *268*, 655–665.
[27] M. H. Parker, P. E. Prevelige, Jr., *Virology* **1998**, *250*, 337–348.
[28] P. R. Weigele, L. Sampson, D. Winn-Stapley, S. R. Casjens, *J. Mol. Biol.* **2005**, *348*, 831–844.
[29] R. Tuma, M. H. Parker, P. Weigele, L. Sampson, Y. Sun, N. R. Krishna, S. Casjens, G. J. Thomas, Jr., P. E. Prevelige, Jr., *J. Mol. Biol.* **1998**, *281*, 81–94.

Received: September 17, 2007
Published online on January 21, 2008

